

Protein Structure *in Vacuo*: Gas-Phase Conformations of BPTI and Cytochrome *c*

Konstantin B. Shelimov,[†] David E. Clemmer,[‡] Robert R. Hudgins, and Martin F. Jarrold*

Contribution from the Department of Chemistry, Northwestern University, 2145 Sheridan Road, Evanston, Illinois 60208

Received June 6, 1996[⊗]

Abstract: Ion mobility measurements have been used to examine the geometries of naked BPTI (bovine pancreatic trypsin inhibitor) and cytochrome *c* ions in the gas phase, as a function of charge. For BPTI, the measured cross sections are close to those estimated for the native solution-phase conformation. Furthermore, gas-phase BPTI retains its compact structure when collisionally heated. These results are consistent with the known stability of BPTI, where the three-dimensional structure is partly locked into place by three covalent disulfide bridges. For cytochrome *c*, geometries with cross sections close to those estimated for the native solution phase structure were observed for the low charge states. For intermediate charge states, the compact geometries are metastable, and when collisionally heated they gradually unfold, through a series of well-defined intermediates. Only extended conformations are observed for the higher charge states, and they become more extended as the charge increases. The gas-phase conformation of a protein ion results from a balance between attractive intramolecular interactions, intramolecular charge “solvation”, and Coulomb repulsion. For the low charge states, compact folded conformations have the lowest energy because they maximize intramolecular interactions. For intermediate charge states, elongated conformations, which minimize Coulomb repulsion while maximizing intramolecular interactions and intramolecular charge “solvation”, become favored. For the high charge states, the elongated conformations unravel to an extended string as Coulomb repulsion dominates.

I. Introduction

Understanding how a protein folds from a random coil to a specific, biologically-active conformation and discerning the relationship between the three-dimensional structure of a protein and its amino acid sequence are important unresolved issues.¹ The complex nature of protein structure and folding makes these problems difficult to understand. There are not only interactions within the protein,^{2,3} but the protein interacts with, and orders the surrounding solvent.⁴ Recent technological developments⁵ now make it possible to study relatively large proteins in the gas phase, free of solvent interactions. While the gas phase may seem to be an unusual environment for studies of protein structure and folding,⁶ these studies allow one to isolate and explore the intramolecular interactions within a protein. In addition, studies of gas-phase proteins solvated with a particular number of water molecules have recently been performed,⁷ and

these studies should provide detailed information about how a protein interacts with its solvent.

The techniques that make it possible to obtain intact biological molecules in the gas phase⁵ were developed to exploit the biological applications of mass spectrometry. These applications now include the sensitive analytical determination of biomolecules, accurate measurements of molecular weights, and sequence information.⁸ In the last couple of years, several different techniques have been employed in an effort to obtain information about the conformations of large biomolecules in the gas phase. Smith, McLafferty, Williams, Cassady, and their collaborators have employed H/D exchange kinetics^{9–12} or proton-transfer kinetics.^{13,14} Douglas, Cooks, and their collaborators have used ion beam scattering to determine collision cross sections for gas-phase protein ions.^{15–17} Sundqvist and

[†] Present address: Department of Chemistry, Rice University, Houston, TX 77251.

[‡] Present address: Department of Chemistry, University of Indiana, Bloomington, IN 47405.

[⊗] Abstract published in *Advance ACS Abstracts*, February 1, 1997.

(1) See for example: Richards, F. M. *Sci. Am.* **1991**, *January*, 54. *Protein Folding*, Creighton, T. E., Ed.; Freeman: New York, 1992. Karplus, M.; Sali, A. *Curr. Opin. Struct. Biol.* **1995**, *5*, 58. Thirumalai, D.; Woodson, S. A. *Acc. Chem. Res.* **1996**, *29*, 433.

(2) Lazaridis, T.; Archontis, G.; Karplus, M. *Adv. Protein Chem.* **1995**, *47*, 231.

(3) Makhatadze, G. I.; Privalov, P. L. *Adv. Protein Chem.* **1995**, *47*, 307.

(4) Rupley, J. A.; Gratton, E.; Careri, G. *Trends Biochem. Sci.* **1983**, *8*, 18. Steinbach, P. J.; Brooks, B. R. *Proc. Natl. Acad. Sci. U.S.A.* **1993**, *90*, 9135. Rupley, J. A.; Careri, G. *Adv. Protein Chem.* **1991**, *41*, 37. van Gunsteren, W. F.; Luque, F. J.; Timms, D.; Torda, A. E. *Annu. Rev. Biophys. Biomol. Struct.* **1994**, *23*, 847.

(5) Monaghan, J. J.; Barber, M.; Bordolom, R.; Sedgewick, E.; Taylor, A. *Org. Mass Spectrom.* **1982**, *17*, 596. Whitehouse, C. M.; Dreyer, R. N.; Yamashita, M.; Fenn, J. B. *Anal. Chem.* **1985**, *57*, 675. Karas, M.; Hillenkamp, F. *Anal. Chem.* **1988**, *60*, 2299.

(6) Wolynes, P. G. *Proc. Natl. Acad. Sci. U.S.A.* **1995**, *92*, 2426.

(7) Woenckhaus, J.; Mao, Y.; Ratner, M. A.; Jarrold, M. F. *J. Phys. Chem.* In press.

(8) See for example: Biemann, K. *Annu. Rev. Biochem.*, **1992**, *61*, 977. Burlingame, A. L.; Boyd, R. K.; Gaskell, S. J. *Anal. Chem.* **1994**, *66*, 634R. Bahr, U.; Karas, M.; Hillenkamp, F. *Fresenius J. Anal. Chem.* **1994**, *348*, 783. Kaufmann, R. *J. Biotechnol.* **1995**, *41*, 155. Chait, B. T.; Kent, S. B. K. *Science* **1992**, *257*, 1885. Chait, B. K.; Wong, R.; Beavis, R. C.; Kent, S. B. H. *Science* **1993**, *262*, 89.

(9) Winger, B. E.; Light-Wahl, K. J.; Rockwood, A. L.; Smith, R. D. *J. Am. Chem. Soc.* **1992**, *114*, 5897.

(10) Suckau, D.; Shi, Y.; Beu, S. C.; Senko, M. W.; Quinn, J. P.; Wampler, F. M.; McLafferty, F. W. *Proc. Natl. Acad. Sci. U.S.A.* **1993**, *90*, 790.

(11) Wood, T. D.; Chorush, R. A.; Wampler, F. M.; Little, D. P.; O'Connor, P. B.; McLafferty, F. W. *Proc. Natl. Acad. Sci. U.S.A.* **1995**, *92*, 2451.

(12) Cassady, C. J.; Carr, S. R. *J. Mass Spectrom.* **1996**, *31*, 247.

(13) Gross, D. S.; Schnier, P. D.; Rodriguez-Cruz, S. E.; Fagerquist, C. K.; Williams, E. R. *Proc. Natl. Acad. Sci. U.S.A.* **1996**, *93*, 3143.

(14) Schnier, P. D.; Gross, D. S.; Williams, E. R. *J. Am. Chem. Soc.* **1995**, *117*, 6747.

(15) Covey, T. R.; Douglas, D. J. *J. Am. Soc. Mass Spectrom.* **1993**, *4*, 616.

(16) Collings, B. A.; Douglas, D. J. *J. Am. Chem. Soc.* **1996**, *118*, 4488.

collaborators have employed scanning probe microscopy of the defects created by the impact of protein ions on surfaces.¹⁸ In the studies described here we have used gas-phase ion mobility measurements to study the conformations of BPTI (bovine pancreatic trypsin inhibitor) and cytochrome *c* as a function of charge state. The mobility of a gas-phase ion depends on its average collision cross section,¹⁹ and so ion mobility measurements can resolve structural isomers and provide an accurate measure of their average cross sections. The cross sections can then be used to deduce information about the geometries present in the gas phase.^{20–22} We have previously shown that ion mobility measurements can resolve a number of conformations for cytochrome *c*,²³ and we have recently described evidence showing that cytochrome *c* ions can spontaneously fold in the gas phase.²⁴ Bowers and collaborators have reported ion mobility measurements for the peptide bradykinin along with extensive molecular dynamics studies.²⁵ Several other groups have also performed ion mobility measurements for biological molecules,²⁶ though no effort was made to deduce structural information in this work.

BPTI was selected for the studies reported here because it is a small protein, 58 residues, in which the three-dimensional structure is partially locked into place by three covalent disulfide bridges. BPTI is very stable against thermal, acid, or base denaturation. Thus we expect the structure of gas-phase BPTI to be quite similar to its native conformation. On the other hand, cytochrome *c* is a small protein, 104 residues, in which there are no disulfide bridges. So cytochrome *c* is relatively free to adopt conformations that are quite different from the native conformation, if such conformations are favored in the gas phase.

II. Experimental Methods

A schematic diagram of the injected ion drift tube apparatus used in these studies is shown in Figure 1.²⁷ The protein ions were generated with an electrospray ion source similar to that described by Smith *et*

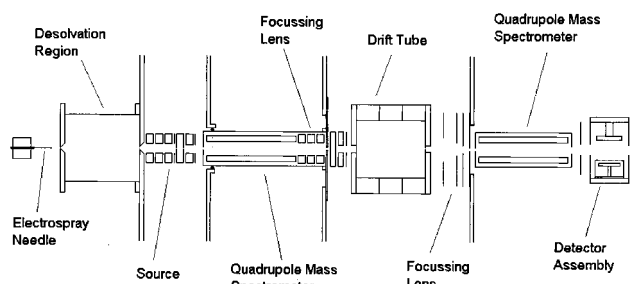


Figure 1. Schematic diagram of the experimental apparatus.

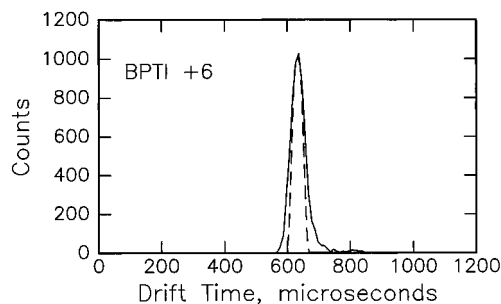


Figure 2. Drift time distribution recorded for the +6 charge state of BPTI. The distribution was recorded with a drift field of 13.16 V/cm, a helium buffer gas pressure of 3.335 Torr, and an injection energy of 900 eV. The dashed line shows the distribution expected for a single conformation (see text).

*al.*²⁸ The electrosprayed solutions were generally around 5×10^{-4} M BPTI or bovine cytochrome *c* (Sigma Chemical Company) in a 75/25 mixture of water and acetonitrile, acidified with 0–4% acetic acid. The needle was operated at 4–5 kV. The solutions were electrosprayed in air, and the ions enter the apparatus through a 0.012-cm-diameter aperture into a desolvation region which may be heated up to 200 °C. The ions are then carried through a 0.625-cm-diameter aperture into the source vacuum chamber which is pumped by three Edwards Diffstak 250 diffusion pumps with a combined pumping speed of 6000 L s⁻¹. Because of this large pumping capacity, it is not necessary to differentially pump the electrospray source. Ions which exit the desolvation region are focussed, with a simple three-element zoom lens, into a quadrupole mass spectrometer, where a particular mass-to-charge ratio is selected. The ions are then focussed into a low energy ion beam and injected into the drift tube. The drift tube is 7.6 cm long with 0.025-cm-diameter entrance and exit apertures. It was operated with helium buffer gas at a pressure of 2–5 Torr. Ions travel across the drift tube under the influence of a 6.58–13.16 V/cm electric field, and a small fraction exits at the other side. The exiting ions are focussed into a second quadrupole mass spectrometer, and at the end of this quadrupole they are detected by an off-axis collision dynode and dual microchannel plates. Ion mobilities were measured by injecting 10–50- μ s pulses of ions into the drift tube and recording their arrival time distribution at the detector using a multichannel scaler. The drift time distribution was then obtained by correcting the time scale so that it only reflects the amount of time spent traveling across the drift tube. In a number of cases, drift time distributions were measured as a function of the drift field to confirm that the drift field was sufficiently low that the measured mobilities were independent of the field strength.

III. Results

A. Bovine Pancreatic Trypsin Inhibitor. Electrospray ionization of BPTI generates ions mainly in the +5 to +7 charge states. We assume that the charge results mainly from the addition of 5–7 protons to BPTI. However, our mass spectrometers are not configured to perform the accurate absolute mass measurements necessary to confirm this. Figure 2 shows a drift time distribution recorded for BPTI in the +6 charge

(17) Cox, K. A.; Julian, R. K.; Cooks, R. G.; Kaiser, R. E. *J. Am. Soc. Mass Spectrom.* **1994**, *5*, 127.

(18) Quist, A. P.; Ahlbom, J.; Reimann, C. T.; Sundqvist, B. U. R. *Nucl. Instr. Meth. Phys. Res. B* **1994**, *88*, 164. Sullivan, P. A.; Axelsson, J.; Altmann, S.; Quist, A. P.; Sundqvist, B. U. R.; Reinmann, C. T. *J. Am. Soc. Mass Spectrom.* **1996**, *7*, 329.

(19) Hagen, D. F. *Anal. Chem.* **1979**, *51*, 870. Karpas, Z.; Cohen, M. J.; Stimac, R. M.; Wernlund, R. F. *Int. J. Mass Spectrom. Ion Proc.* **1986**, *83*, 163. von Helden, G.; Hsu, M. T.; Kemper, P. R.; Bowers, M. T. *J. Chem. Phys.* **1991**, *95*, 3835. For a recent review see, St. Louis, R. H.; Hill, H. H. *Crit. Rev. Anal. Chem.* **1990**, *21*, 321.

(20) Lin, S. T.; Griffin, G. W.; Horning, E. C.; Wentworth, W. E. *J. Chem. Phys.* **1974**, *60*, 4994.

(21) Jarrold, M. F.; Constant, V. A. *Phys. Rev. Lett.* **1992**, *67*, 2994. Clemmer, D. E.; Hunter, J. M.; Shelimov, K. B.; Jarrold, M. F. *Nature* **1994**, *372* 248. Hunter, J. M.; Fye, J. L.; Jarrold, M. F.; Bower, J. E. *Phys. Rev. Lett.* **1994**, *73* 2063. Hunter, J. M.; Jarrold, M. F. *J. Am. Chem. Soc.* **1995**, *117* 10317. Jarrold, M. F. *J. Phys. Chem.* **1995**, *99* 15. Shelimov, K. B.; Clemmer, D. E.; Jarrold, M. F. *J. Chem. Soc. Dalton* **1996**, 567.

(22) von Helden, G.; Hsu, M.-T.; Gotts, N.; Bowers, M. T. *J. Phys. Chem.* **1993**, *97*, 8182. von Helden, G.; Gotts, N. G.; Maitre, P.; Bowers, M. T. *Chem. Phys. Lett.* **1994**, *227*, 601. von Helden, G.; Wyttenbach, T.; Bowers, M. T. *Int. J. Mass Spectrom. Ion Proc.* **1995**, *146/147*, 349. Lee, S.; Wyttenbach, T.; von Helden, G.; Bowers, M. T. *J. Am. Chem. Soc.* **1995**, *117*, 10159.

(23) Clemmer, D. E.; Hudgins, R. R.; Jarrold, M. F. *J. Am. Chem. Soc.* **1995**, *117*, 10141.

(24) Shelimov, K. B.; Jarrold, M. F. *J. Am. Chem. Soc.* In press.

(25) von Helden, G.; Wyttenbach, T.; Bowers, M. T. *Science* **1995**, *267*, 1483. Wyttenbach, T.; von Helden, G.; Bowers, M. T. *J. Am. Chem. Soc.* **1996**, *118*, 8355.

(26) Smith, R. D.; Loo, J. A.; Loo, R. R.; Busman, M.; Udseth, H. R. *Mass Spectrom. Rev.* **1991**, *10*, 359. Smith, R. D.; Loo, J. A.; Loo, R. R.; Udseth, H. R. *Mass Spectrom. Rev.* **1992**, *11*, 434. Wittmer, D.; Chen, Y. H.; Luckenbill, B. K.; Hill, H. H. *Anal. Chem.* **1994**, *66*, 2348.

(27) Jarrold, M. F.; Bower, J. E.; Creegan, K. *J. Chem. Phys.* **1989**, *90*, 3615. Jarrold, M. F.; Bower, J. E. *J. Chem. Phys.* **1992**, *96*, 9180.

(28) Smith, R. D.; Loo, J. A.; Edmonds, C. G.; Barinaga, C. J.; Udseth, H. R. *Anal. Chem.* **1990**, *62*, 882.

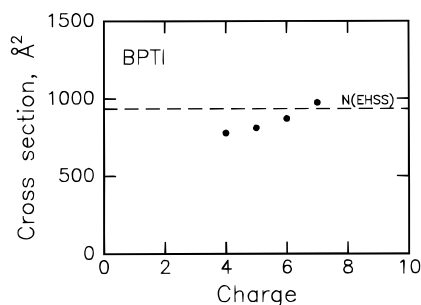


Figure 3. Plot of the average collision cross sections deduced from the ion mobility measurements for BPTI in the +4 to +7 charge states. The dashed line labeled N(EHSS) shows the cross section estimated for BPTI using the exact hard spheres scattering model with crystal structure coordinates (see text).

state. A single, relatively sharp peak is observed. The dashed line in the figure shows the drift time distribution obtained from solution of the transport equation for a single conformation in the drift tube.²⁹ The measured distribution is slightly broader than the calculated one. Similar deviations were found for the other charge states of BPTI. These results indicate that BPTI does not have a single geometry in the gas phase, but exists in a number of closely related conformations. The average cross section, or more precisely the orientationally averaged collision integral, $\Omega_{\text{avg}}^{1,1}$ can be deduced from the drift time using^{29,30}

$$\Omega_{\text{avg}}^{1,1} = \frac{(18\pi)^{1/2}}{16} \left[\frac{1}{m} + \frac{1}{m_B} \right]^{1/2} \frac{ze}{(k_B T)^{1/2}} \frac{t_D E}{L \rho} \quad (1)$$

In this expression m is the mass of the ion, m_B is the mass of a buffer gas atom, ρ is the buffer gas number density, L is the length of the drift tube, E is the electric field, and t_D is the drift time. Figure 3 shows the average cross sections, deduced using this expression, plotted against charge state. The cross sections increase with charge.

As the ions are injected into the drift tube, their kinetic energy is rapidly thermalized, and during this process the injected ions become collisionally heated. As the injection energy is raised, the collisional heating increases, and this can be exploited to examine structural interconversions.²¹ In the present case, raising the injection energy might be expected to result in unfolding. However, no significant changes in the drift time distributions for BPTI were observed for injection energies up to 1500 eV (the injection energy is defined as the voltage difference between the exit of the desolvation region and the entrance of the drift tube multiplied by the charge). This indicates that either BPTI does not unfold or it refolds in less than 100 μs . If an extended conformation was generated and it took more than 100 μs to refold there would be a discernable shift in the position of the peak.

B. Cytochrome *c*. Electrospray ionization of cytochrome *c* generates a distribution of charge states that depends on the pH of the solution.³¹ For a solution with no added acid, the distribution peaks around the +8 charge state. When acid is added the distribution shifts to substantially higher charge states, typically centered around +15 to +16. It has been suggested that this change in the charge state distribution reflects a change in the solution structure of cytochrome *c*. Cytochrome *c* is denatured in acidic solutions, and the substantial increase in

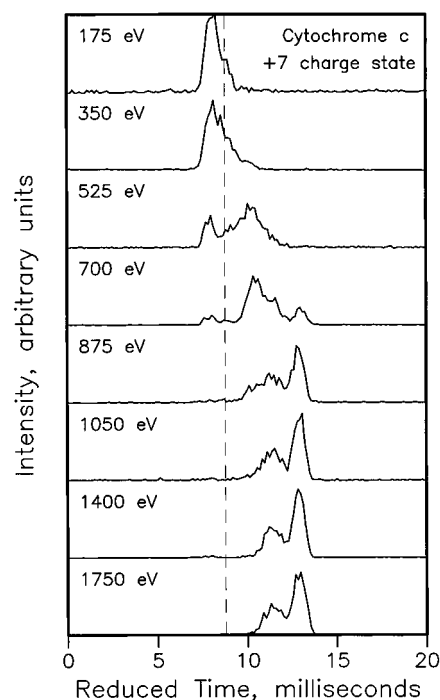


Figure 4. Drift time distributions for the +7 charge state of cytochrome *c* recorded with injection energies of 175–1750 eV. The drift time distributions are plotted against a reduced time scale obtained by multiplying the measured drift times (scaled to a buffer gas pressure of 5 Torr) by the charge. The dashed line shows the reduced drift time determined for the native conformation using the exact hard spheres scattering model (see text).

the average charge probably occurs because more basic sites are available for protonation on the unfolded form.³¹

Figure 4 shows drift time distributions recorded as a function of injection energy for the +7 charge state of cytochrome *c* produced by electrospraying an unacidified solution. The distributions are plotted against a reduced time scale given by the measured drift time multiplied by the charge. This removes the effect of the charge on the drift times, and facilitates comparison between drift time distributions recorded for different charge states. At an injection energy of 175 eV the distribution is dominated by a peak at around 8 ms. For injection energies larger than 1050 eV there are two peaks at around 12 and 13 ms. The ratio of these peaks remains fairly constant for injection energies greater than 1050 eV. This suggests that the relative abundances of the conformations responsible for these peaks has been fixed by an equilibrium during the transient heating and cooling processes that occur as the ions are injected into the drift tube. At injection energies between 175 and 1050 eV the distribution gradually shifts to longer times and several intermediate states are apparent.

There is a concern that as the injection energy is raised the ions may not cool to the buffer gas temperature fast enough, and the drift time distributions may be influenced by residual internal energy. The protein ions typically experience $>10^6$ collisions as they travel across the drift tube. A simple test to determine whether the experimental results are influenced by incomplete cooling is to change the buffer gas pressure or the drift voltage so that the ions spend either more or less time in the drift tube. The drift time distributions did not change significantly. Another issue is whether or not the features observed in the drift time distributions of the intermediate charge states at high injection energies represent the lowest free energy conformations at room temperature. At high injection energies the ions are rapidly heated and cooled, and the conformation

(29) Mason, E. A.; McDaniel, E. W. *Transport Properties of Ions in Gases*; Wiley: New York, 1988.

(30) Hirschfelder, J. O.; Curtiss, C. F.; Bird, R. B. *Molecular Theory of Gases and Liquids*; Wiley, New York, 1954.

(31) Chowdhury, S. K.; Katta, V.; Chait, B. T. *J. Am. Chem. Soc.* **1990**, *112*, 9012.

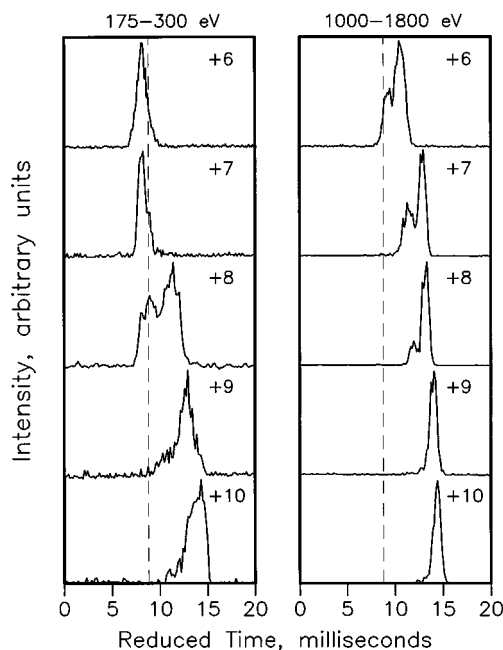


Figure 5. Drift time distributions recorded for +6 to +10 charge states of cytochrome *c*, generated by electro spraying an unacidified solution. The distributions on the left were measured with low injection energies (300, 175, 200, 225, and 250 eV for the +6 to +10 charge states, respectively) and those on the right were recorded at high injection energies (1800, 1750, 1600, 1800, and 1000 eV). The drift time distributions are plotted against a reduced time scale obtained by multiplying the measured drift times (scaled to a pressure of 5 Torr) by the charge. The dashed line shows the reduced drift time determined for the native conformation using the exact hard spheres scattering model (see text).

that dominates under these conditions is the one that dominates when the rate of isomerization becomes sufficiently small that the isomer distribution is frozen. This may occur at high temperatures, and the isomer that dominates at high temperature is not necessarily the one that has the lowest free energy at room temperature.

Figure 5 shows drift time distributions measured for the +6 to +10 charge states of cytochrome *c*, generated by electro spraying an unacidified solution. Distributions recorded at low (175–300 eV) and high (1000–1800 eV) injection energies are shown. The low injection energy data represent the isomer distributions generated in the electrospray source. The +6 and +7 charge states have peaks at a reduced time of around 8 ms. These peaks are substantially broader than expected for a single conformation. For the +8 charge state the distribution is very broad and consists of a number of unresolved peaks. For the higher charge states the distributions narrow and peak at longer drift times. At high injection energies, all the drift time distributions shift to longer times and for the higher charge states they become dominated by a single relatively narrow peak. To obtain charge states higher than +10 in substantial amounts, it is necessary to electro spray an acidified solution. Drift time distributions recorded for the +11 to +20 charge states produced by electro spraying a solution acidified with 2.5% acetic acid show a single peak similar to that observed for the +10 charge state at high injection energy (see Figure 5). The peak gradually shifts to longer drift times with increasing charge.

Charge states below +6 were obtained by proton stripping reactions^{11,13} with a base introduced into the desolvation region. The desolvation region was heated to 120–150 °C for these studies. With MTBD (1,3,4,6,7,8-hexahydro-1-methyl-2*H*-pyrimido[1,2-*a*]pyrimidine, Aldrich Chemical Company) charge states as low as +3 can be produced.¹⁴ Figure 6 shows drift

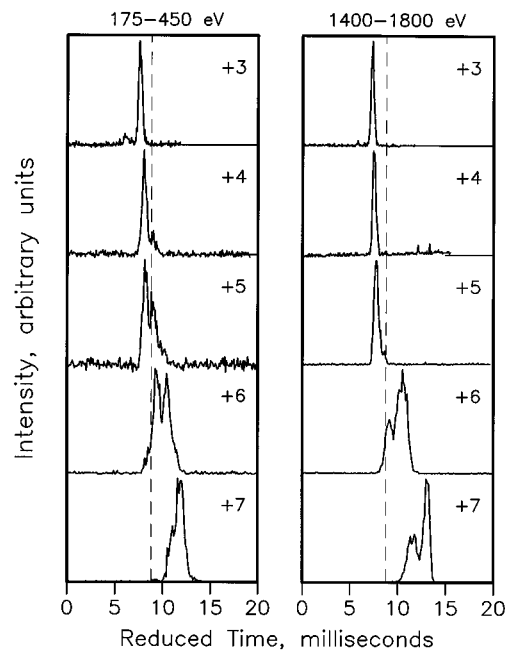


Figure 6. Drift time distributions recorded for +3 to +7 charge states of cytochrome *c*, generated by charge stripping high charge states by MTBD. The distributions on the left were measured at low injection energies (450, 200, 250, 300, and 175 eV for the +3 to +7 charge states, respectively) and those on the right were recorded at high injection energies (1500, 1400, 1500, 1800, and 1750 eV). The drift time distributions are plotted against a reduced time scale obtained by multiplying the measured drift times (scaled to a pressure of 5 Torr) by the charge. The dashed line shows the reduced drift time determined for the native conformation using the exact hard spheres scattering model (see text).

time distributions recorded for the +3 to +7 charge states generated by proton stripping the high charge states produced by electro spraying a solution acidified with 2.5% acetic acid. With 2.5% acetic acid the charge distribution peaks at around +14, and the lowest charge state observed, without the base in the desolvation region, is +8. The drift time distributions measured for the higher charge states under these conditions show a single relatively narrow peak with reduced drift times >14 ms. The distributions on the left in Figure 6 were recorded with low injection energies while those on the right were recorded with high injection energies. For the lower charge states, +3 to +5, the drift time distributions show a peak at around 8 ms. These peaks shift to slightly shorter time as the injection energy is increased. For the +6 and +7 charge states the distributions at low injection energies are different from those generated by direct electrospray ionization of unacidified solutions, they are shifted to longer times. However, at high injection energies the distributions are identical to those recorded with an unacidified solution.

Figure 7 shows a plot of the collision cross sections, determined using eq 1, for the main features resolved in the drift time distributions of the +3 to +20 charge states. The filled points show cross sections for the features that dominate at high injection energies and the open points show cross sections for features observed at other injection energies. For the intermediate charge states it appears that similar conformations coexist for several charge states. Depending on the charge, these conformations may be stable or metastable. The cross sections for each conformation systematically increase with charge. The cross sections reported here for the intermediate and high charge states are in qualitative agreement with cross sections determined from ion beam scattering experiments.¹⁵ However, the ion beam scattering experiments were not able

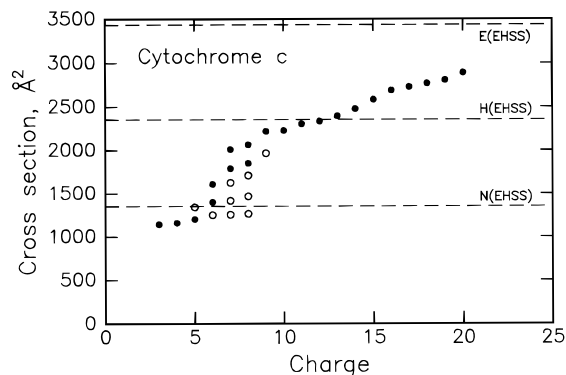


Figure 7. Plot of the cross sections determined for the main features resolved in the drift time distributions for the +3 to +20 charge states of cytochrome *c*. Cross sections for the features that dominate at high injection energies are shown by the filled points. The open points show the cross sections deduced for conformations observed at lower injection energies. The dashed lines labelled N(EHSS), H(EHSS), and E(EHSS) show the cross sections determined using the exact hard spheres scattering model for the native conformation, an α -helix, and an extended string, respectively (see text).

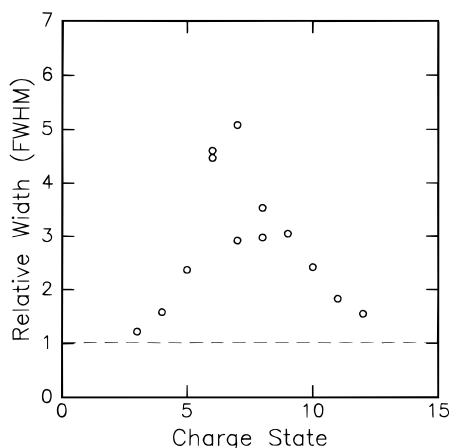


Figure 8. The relative widths (the measured width (fwhm) divided by the width calculated for a single conformation) for the features observed in the drift time distributions for cytochrome *c* at high injection energies, plotted against charge state.

to resolve the different conformations observed in the ion mobility experiments at low injection energies.

Figure 8 shows the relative widths of the peaks in the drift time distributions, recorded at high injection energies, plotted against the charge state. The relative widths are obtained by dividing the measured widths (fwhm) by those calculated for a single conformation from the transport equation for ions in the drift tube.²⁹ For the low charge states, the relative widths are close to one. The widths increase significantly for intermediate charge states and then decrease to approach one again. This indicates that the low and high charge states are dominated by a few closely related conformations while for the intermediate charge states a broader range of conformations is present.

IV. Discussion

A. Comparison with Cross Sections Calculated for Specific Conformations. Information about the conformations resolved in the ion mobility measurements can be obtained by comparing the measured cross sections to those calculated for specific conformations.²⁰ In virtually all of the previous ion mobility studies a simple hard sphere projection approximation was employed to estimate the cross sections.^{21,22} With this model, the cross section is given by the average size, or more

precisely, by the orientationally averaged area eclipsed by the trial geometry in collisions with the buffer gas. The implementation of this model requires hard sphere contact distances between helium and the atoms in the protein. We employed 2.2 Å for He–H interactions and 2.7 Å for all the other atoms. Cross sections were estimated for BPTI using coordinates obtained from the Protein Data Bank.³² Three slightly different crystal structures have been reported for BPTI.^{33–35} For crystal structure **II** (5PTI) the cross section estimated using the simple projection approximation is 767 Å². Coordinates for the other two crystal structures and NMR solution structure coordinates³⁶ give similar values.

The cross section, or more correctly the collision integral, in eq 1 should be obtained by averaging the momentum transfer cross section over the relative velocity and collision geometry.^{29,30,37} The momentum transfer cross section is a function of the scattering angle, the angle between the incoming and outgoing trajectory in a collision between the buffer gas atom and the protein. The simple projection approximation ignores all these details. Shvartsburg and Jarrold³⁸ have recently described a model which treats the scattering correctly, within the hard sphere limit, and they have shown that the simple projection approximation can substantially underestimate the collision integral for some geometries. The collision integral determined for BPTI using the exact hard spheres scattering model and the coordinates for crystal structure **II** is 935 Å². This is 22% larger than the cross section determined from the simple projection model. Thus it appears that it is important to treat the scattering correctly when estimating collision integrals for these large protein ions.

Both models described above ignore the long-range interactions between the protein ion and buffer gas atom. Since the protein is relatively highly charged, ion-induced dipole interactions might be expected to make a significant contribution to the collision integral. To obtain an estimate of the effect of the ion-induced dipole interactions, we have calculated collision integrals for a hard sphere plus ion-induced dipole potential from an analytical solution of the equations of motion. For a sphere of the same average size as BPTI, addition of the ion-induced dipole potential causes only a relatively small increase in the collision integral, from 767 Å² for an uncharged sphere to 784 Å² for a sphere with 10 charges. The increase is small because of the large physical size of the protein and the small polarizability of helium.

The dashed line in Figure 3 labelled N(EHSS) shows the collision integral determined for the native structure using the exact hard spheres scattering model. The measured cross sections for the lower charge states of BPTI are significantly smaller than the cross section estimated for the native conformation. This indicates that the lower charge states are more compact in the gas phase than in solution. Globular proteins such as BPTI are compact objects, but they are not close-packed. The solvent provides an average external force field which prevents the protein from packing tightly, and in solution, globular proteins contain cavities large enough to accommodate water molecules, and the polar side chains extend into the

(32) <http://www.pdb.bnl.gov>.

(33) Deisenhofer, J.; Steigemann, W.; *Acta Crystallogr.* **1975**, *31*, 238.

(34) Wlodawer, A.; Walter, J.; Huber, R.; Sjolin, L. *J. Mol. Biol.* **1984**, *180*, 301.

(35) Wlodawer, A.; Nachman, J.; Gilliland, G. L.; Gallagher, W.; Woodward, C. *J. Mol. Biol.* **1987**, *198*, 469.

(36) Berndt, K. D.; Guntert, P.; Orbons, L. P. M.; Wuthrich, K. *J. Mol. Biol.* **1992**, *227*, 757.

(37) Mesleh, M. F.; Hunter, J. M.; Shvartsburg, A. A.; Schatz, G. C.; Jarrold, M. F. *J. Phys. Chem.* **1996**, *100*, 16082.

(38) Shvartsburg, A. A.; Jarrold, M. F. *Chem. Phys. Lett.* **1996**, *261*, 86.

solvent to maximize solvation. In the absence of the solvent, intramolecular interactions make the protein pack more tightly, and the polar side chains collapse onto the protein surface. According to molecular dynamics simulations performed for BPTI *in vacuo*, in a crystal, and in a solvent^{39,40} the radius of gyration decreases by 5.1–5.3% when the solvent is removed, and by 7.7% on going from the crystal to vacuum. Such changes are expected to result in a 10–16% decrease in the cross section estimated using the projection approximation, and a slightly larger decrease in the cross section determined by the exact hard spheres scattering model.⁴¹ This will bring the cross section obtained from the exact hard spheres scattering model close to the cross sections measured for the lower charge states of BPTI.

The collision integral determined for the native conformation of cytochrome *c* from the exact hard spheres scattering model is 1339 Å². X-ray crystal structure coordinates⁴² and the NMR solution structure coordinates,⁴³ obtained from the Protein Data Bank,³² give similar values. The projection approximation yields a value of 1075 Å². The value obtained from the projection approximation was employed in preliminary accounts of this work.^{23,24} However, it is now clear that this model substantially underestimates the collision integral for these large protein ions. The dashed line in Figure 7 labeled N(EHSS) shows the cross section predicted for the native conformation using the exact hard spheres scattering model. The measured cross sections for the most compact conformation observed for the low charge states of cytochrome *c* are slightly smaller than the cross section for the native conformation. This is consistent with the gas phase protein being slightly more compact than in solution. An extended form of cytochrome *c*, a nearly linear string, can be obtained by setting all Φ and Ψ angles (except those between Cys14 and Cys17 where the heme is covalently bound) to 180°, and adjusting the torsion angles near the proline residues. The collision integral determined for this linear string using the exact hard spheres scattering model is 3453 Å². The dashed line in Figure 7 labeled E(EHSS) shows the cross section for this extended conformation. The cross sections determined for the higher charge states approach this limiting value. The cross section determined using the exact hard spheres scattering model for cytochrome *c* in a completely α -helical conformation, generated by setting all Φ angles to -57° and all Ψ angles to -47° , is 2351 Å². The dashed line in Figure 7 labeled H(EHSS) shows the cross section obtained for the α -helix. It is close to the cross sections determined for the +11 to +13 charge states.

B. Unfolding and Refolding of Cytochrome *c*. The results described above indicate that BPTI retains most of its compact folded conformation in the gas phase even when collisionally heated. This is presumably because its three-dimensional structure is partly locked into place by three covalent disulfide bridges. For cytochrome *c*, compact conformations with cross sections close to that expected for a collapsed native conformation were observed at low injection energies for the +6 and +7 charge states generated by direct electrospray ionization of

unacidified solutions (see Figure 7). A collapsed native conformation, which has a high density of van der Waals contacts and hydrogen bonds, is expected to be stable in vacuum, and the observation of these compact conformations from an unacidified solution indicates that electrospray ionization is capable of retaining the main features of the solution phase structure of a protein without disulfide bridges. However, when collisionally heated these compact conformations unfold (see Figure 4). If the +6 and +7 charge states are produced by charge stripping from high charge states that are unfolded, they remain unfolded, at least on the time scale of our experiments (see Figure 6). In contrast, the +3 to +5 charge states generated by proton stripping from unfolded high charge states have cross sections close to that expected for the native conformation. Thus the low charge states must have folded in the gas phase after the proton stripping reactions.²⁴ The peaks for these charge states become narrower and shift to slightly shorter times when the injection energy is raised. This indicates that the folded conformations generated in the initial collapse after proton stripping become more compact when collisionally heated, which in turn suggests that there is an activation barrier for generating the most compact conformation. While disordered compact conformations may result from the spontaneous collapse of an extended geometry, the annealing of the initial collapsed structures into more compact conformations and the small widths of the corresponding peaks in the drift time distributions suggest that the resulting conformations are not disordered. Although these features have cross sections close to that expected for the native conformation, this does not necessarily mean that they have this structure. A collapsed native structure is expected to be stable in the gas phase. However, the kinetic accessibility of the native state in the absence of a polar solvent is questionable. Furthermore, it may not be the most stable compact gas-phase conformation. An ordered conformation with a core of polar residues on the inside and nonpolar residues on the outside (the so-called “inside-out protein”⁶) may be a viable alternative to a collapsed native geometry. Structures of this type should be highly stable in the gas phase and may be kinetically accessible. On the other hand, the sequences of proteins that have evolved in an aqueous environment may be incompatible with the inside-out geometry.

C. Comparison with H/D Exchange Results. McLafferty and collaborators¹¹ have reported two studies of cytochrome *c* ions in the gas phase using H/D exchange kinetics. In these studies it is assumed that the number of exchangeable hydrogens can be correlated with the exposed surface area of the protein. Several exchange levels were found for the +7 and +8 charge states indicating the presence of several conformations. This is consistent with the ion mobility results presented here. However, the exchange levels do not increase significantly for the higher charge states. The exchange levels for all charge states from +8 to +16 are similar, while we observe a substantial increase in the cross sections over this range. McLafferty and collaborators have also performed some collisional heating and charge stripping studies. They found that the H/D exchange level increased substantially when the +12 to +15 charge states were collisionally heated, and that charge stripping the +15 charge state to +7 more than halved the H/D exchange level, to a value lower than that obtained for the +7 charge state generated by direct electrospray ionization. These results differ from our observations for charge stripping and collisional heating; however, some of these differences could result from different experimental conditions and different experimental time scales. On the other hand, recent studies by

(39) van Gunsteren, W. F.; Karplus, M. *Biochemistry* **1982**, *21*, 2259.

(40) Levitt, M.; Sharon, R. *Proc. Natl. Acad. Sci. U.S.A.* **1988**, *85*, 7557.

(41) The deviations between the cross sections determined by the projection approximation and the exact hard spheres scattering model result from the effects of multiple scattering. Multiple scattering occurs because the surface of the protein is rough and has cavities. For a smooth body with no concave surfaces, the exact hard spheres scattering model and the projection approximation yield identical results. Thus as the protein contracts and the cavities on its surface close up the difference between the cross sections predicted by the projection approximation and the exact hard spheres scattering model will become smaller.

(42) Bushnell, G. W.; Louie, G. V.; Brayer, G. D. *J. Mol. Biol.* **1990**, *214*, 585.

(43) Qi, P. X.; DiStefano, D. L.; Wand, A. *J. Biochem.* **1994**, *33*, 6408.

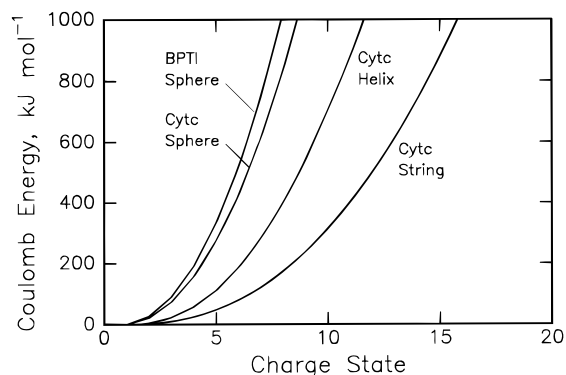


Figure 9. Plot of the Coulomb energy of spheres with the same average size as native BPTI and native cytochrome *c*. The estimated Coulomb energy of cytochrome *c* as an α -helix and a fully extended string are shown for comparison. All calculations were performed using a dielectric constant of 2.0.

Beauchamp and collaborators⁴⁴ indicate that gas-phase H/D exchange is a highly complex process even for simple model peptides, and they suggest that “any temptation to assign gas-phase structures of biological molecules from H/D exchange results must be approached with caution”.

D. The Role of Coulomb Repulsion. In the absence of a solvent with a high dielectric constant (water has a dielectric constant of around 80⁴⁵) Coulomb repulsion becomes substantially more important.⁴⁶ In order to estimate Coulomb energies for multiply charged protein ions it is necessary to have a value for the dielectric constant for the protein to account for shielding of the charge by the protein itself. Some recent work suggests that a dielectric constant of around 2.0 is appropriate for gas-phase cytochrome *c*,¹⁴ and we have used this value here. An estimate of the magnitude of the Coulomb energies was obtained for the native conformations by assuming that the charges are distributed over the surface of a sphere of the same average size as the native protein. Figure 9 shows a plot of the Coulomb energies for BPTI and cytochrome *c* as a function of charge. The Coulomb energy increases rapidly as the charge increases and for the +7 charge state of BPTI it is around 748 kJ mol⁻¹, according to the simple model employed here. This provides a large incentive for BPTI to expand to minimize its Coulomb energy. And so Coulomb repulsion probably accounts for the increase in the cross sections observed for BPTI as the charge increases.

In contrast to BPTI, cytochrome *c* conformations with drift times close to that expected for the native conformation are only observed for the low charge states. The cross sections for the low charge states increase with increasing charge presumably because of Coulomb repulsion. However, cytochrome *c* is not constrained by disulfide bridges, and higher charge states can unfold to reduce Coulomb repulsion. It is apparent from Figure 7 that a sharp unfolding transition occurs for the intermediate charge states of cytochrome *c* as the charge increases. This unfolding transition is somewhat analogous to acid denaturation in solution. In solution, the average charge on cytochrome *c* at pH 7 is $\sim +5$ for the reduced form and $\sim +6$ for the oxidized form.⁴⁷ As the pH is lowered, the charge increases to $\sim +11$

and $\sim +12$ at pH 4. Below pH 4 cytochrome *c* denatures.⁴⁸ Native cytochrome *c* in solution can tolerate higher charge states than the compact conformations in the gas phase because it is in a liquid with a high dielectric constant.

The best geometry for minimizing Coulomb repulsion is an elongated one. Scanning probe microscopy studies of the defects generated by high energy impact of highly charged apomyoglobin ions on graphite suggest that these ions adopt elongated geometries.¹⁸ Coulomb energies estimated for a fully extended form of cytochrome *c*, a linear string, are shown in Figure 9. These values were determined by distributing the charges along the length of the string in the minimum energy configuration. The difference between the Coulomb energies for the native and string forms provides a measure of the Coulomb forces driving the protein to adopt a more extended conformation. This difference is 64 kJ mol⁻¹ for the +3 charge state, 492 kJ mol⁻¹ for the +7 charge state, and 4620 kJ mol⁻¹ for the +20 charge state. So it is easy to understand why the protein unfolds as the charge increases.

E. The Balance between Coulomb Repulsion and Intramolecular Interactions and the Conformations of the Intermediate Charge States. The decrease in the Coulomb energy on going to a more extended conformation is offset by the loss of intramolecular interactions which stabilize the more compact conformations. The folding free energy for cytochrome *c* in solution is -37.1 kJ mol⁻¹ at room temperature.³ The folding free energy *in vacuo* is not known, but it is expected to be much larger because solvation effects balance the intramolecular interactions in solution. A value of -3497 kJ mol⁻¹ for the folding free energy of cytochrome *c* in the gas phase is obtained using the enthalpy (-5261 kJ mol⁻¹) and entropy (-5919 J K⁻¹ mol⁻¹) of folding *in vacuo* determined by Makhatazde and Privalov³ from solution values using the accessible surface area model of solvation. A value of -2182 kJ mol⁻¹ for the folding free energy *in vacuo* is obtained using the enthalpy of folding (-3946 kJ mol⁻¹) determined by Lazaridis et al.² by molecular mechanics modeling with the CHARMM force field, and the entropy of folding determined by Makhatazde and Privalov.³ The larger of these two estimates does not appear to be consistent with our experimental results and the smaller value is employed below.

For the lowest charge states one expects a gas-phase protein to adopt the conformation that maximizes intramolecular interactions, that is the most compact conformation. For the highest charge states, where Coulomb repulsion dominates, the protein is driven to adopt the most extended conformation. For intermediate charge states, a balance must be struck between the Coulomb repulsion and intramolecular interactions, with Coulomb repulsion favoring elongated conformations. An α -helix is a plausible elongated conformation; it reduces Coulomb repulsion, while gaining the energy associated with helix formation. The Coulomb energies estimated for an α -helix are shown in Figure 9.⁴⁹ The α -helix has significantly lower Coulomb energies than the compact folded conformation. The free energy for α -helix formation in the gas phase is around -16.7 kJ mol⁻¹ per residue at 300 K according to a recent theoretical estimate.⁵⁰ Use of this value leads to a free energy of α -helix formation of around -1670 kJ mol⁻¹ for cytochrome *c* at 300 K.

(44) Cambell, S.; Rodgers, M. T.; Marzluff, E. M.; Beauchamp, J. L. *J. Am. Chem. Soc.* **1995**, *117*, 12840.

(45) *Handbook of Chemistry and Physics*; Weast, R. C., Ed.; CRC Press: Boca Raton, 1985.

(46) Wong, S. F.; Meng, C. K.; Fenn, J. B. *J. Phys. Chem.* **1988**, *92*, 546. Nohmi, T.; Fenn, J. B. *J. Am. Chem. Soc.* **1992**, *114*, 3241. Rockwood, A. L.; Busman, M.; Smith, R. D. *Int. J. Mass Spectrom. Ion Proc.* **1991**, *111*, 103.

(47) Theorell, H.; Akesson, A. *J. Am. Chem. Soc.* **1941**, *63*, 1818.

(48) Dickerson, R. E.; Timkovich, R. In *The Enzymes*; Boyer, P. D., Ed.; Academic: New York, 1975; Vol. XIA. Meyer, Y. P.; Saturno, A. F. *J. Protein Chem.* **1990**, *9*, 379.

(49) The Coulomb energies for the α -helix were estimated by distributing the charges in their minimum energy configuration over the surface of a cylinder with approximately the dimensions of an α -helix.

(50) Yang, A.-S.; Honig, B. *J. Mol. Biol.* **1995**, *252*, 351.

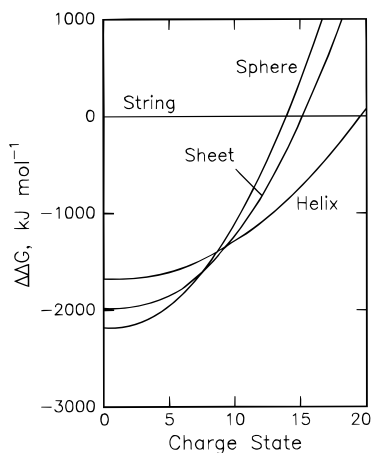


Figure 10. The estimated free energies, including Coulomb interactions, for the native conformation, β -sheet, an α -helix, and an extended string minus the free energy for the extended string, plotted against charge state (see text).

The other classic element of protein secondary structure is a β -sheet. A multistrand antiparallel β -sheet with adjacent strands connected by β -turns is stabilized by backbone hydrogen bonds, and while the number of hydrogen bonds is less than in an α -helix, quantum chemical calculations⁵¹ suggest that hydrogen bonds in a typical β -sheet are stronger, by around 3 kJ mol^{-1} , than in a typical α -helix because they are less strained. For an n -residue polypeptide, the number of backbone hydrogen bonds in an m -strand β -sheet is approximately $(n/m - 2)(m - 1)$. Additional stabilization of β -sheets results from side chain interactions. If two polar residues are next to each other on adjacent strands of a β -sheet, they may form a hydrogen bond. If f_p is the fraction of polar residues in a protein (0.56 for cytochrome *c*), then the number of polar-polar contacts is $(n/m - 2)(m - 1)f_p^2$. Assuming a free energy for hydrogen bond formation of 19.7 kJ mol^{-1} , the free energy for forming the most stable β -sheet is $-1980 \text{ kJ mol}^{-1}$. Thus for an uncharged protein the β -sheet is expected to be more stable than an α -helix. However, the β -sheet is a two-dimensional structure, and its Coulomb energies⁵² lie between those for the native conformation and the α -helix.

Using the estimated folding free energies for the native conformation, the α -helix, and the β -sheet, along with the Coulomb energies estimated for these conformations and the extended string, it is possible to estimate the relative stabilities of these conformations as a function of charge state. These estimates are given in Figure 10, which shows a plot of the free energies, including Coulomb energies, of the native, sheet, helix, and string conformations minus the free energy of the string, as a function of charge. For the low charge states the globular native conformation is the most stable because it has the most favorable intramolecular interactions. For higher charge states the Coulomb energy begins to become significant, and the native conformation, β -sheet, and α -helix all have comparable energies. The model presented in Figure 10 suggests that a sharp sphere \rightarrow sheet \rightarrow helix unfolding transition occurs between the +7 and +9 charge states. Experimentally, an unfolding transition is observed between the +6 and +8 charge states (see Figure 7). The fact that very different geometries have similar energies for the intermediate charge states also explains why a number of different conformations is observed around the unfolding transition. Thus the simple

model presented here correctly predicts both the presence of a sharp unfolding transition and approximately the charge range in which this transition occurs.

The cross section estimated for the α -helix is close to the cross section measured for the most extended conformation observed for the +11 to +13 charge states of cytochrome *c* (see Figure 7). This is consistent with the model presented in Figure 10, which suggests that the α -helix is a favorable conformation for these charge states. Cross sections estimated using the exact hard spheres scattering model for β -sheets with 4–8 strands are $1850\text{--}1950 \text{ \AA}^2$, which is close to the cross section observed for the second most unfolded conformation of the +7 and +8 charge states. While the β -sheet is a favorable gas-phase conformation for these charge states (see Figure 10), this should not be taken to indicate that these features are β -sheets. However, these results do indicate that the conformations observed for the intermediate charge states are partially folded with substantial amounts of secondary structure. There is a large number of plausible partially-folded conformations which could have energies comparable to the geometries discussed here. McLafferty and collaborators¹¹ have attempted to correlate the features they observe in their H/D exchange studies with conformations observed in solution. In view of the much larger role of Coulomb repulsion in the gas phase, it is not obvious to us that a strong correlation should exist between the partially-folded conformations observed in solution and in the gas phase. The absence of detailed structural information for the partially-folded conformations in solution precludes evaluation of their cross sections for comparison with the cross sections measured in the gas phase.

F. Intramolecular Charge “Solvation” and Unfolding of the Higher Charge States. An α -helix is a low energy conformation for the intermediate charge states because it reduces Coulomb repulsion while having favorable intramolecular interactions. However, there is another factor which may play an important role in defining the structure of a protein in the gas phase: intramolecular charge “solvation”. Recent molecular dynamics simulations of protonated bradykinin, a peptide containing nine amino acids, show an intramolecular charge “solvation” shell around the charge site.²⁵ Gas-phase basicities measured for $(\text{Gly})_n$ ($n = 1\text{--}10$),^{53–55} $(\text{Ala})_n$ ($n = 1\text{--}6$),⁵⁴ and other peptides¹⁴ systematically increase with the size of the peptide, and this increase has been attributed to intramolecular charge “solvation”, where residues remote from the charge site “solvate” the charge by coordination to their carbonyl oxygens. The intramolecular “solvation” free energies determined from different studies are not in good agreement. However, all the studies show that the intramolecular “solvation” free energy per residue becomes less negative as the peptide becomes larger. The dependence of the total “solvation” free energy on the size of the peptide can be reasonably parametrized as $SE = C(n_{SS} - 1)^{1/2}$, where n_{SS} is the number of residues in the “solvation” shell and C is a constant with a value of -29 kJ mol^{-1} . Using this expression, the intramolecular charge “solvation” energy for the +7 charge state of cytochrome *c* is estimated to be around -760 kJ mol^{-1} . This is considerably less negative than the $-1670 \text{ kJ mol}^{-1}$ associated with the formation of an α -helix. Note that for small singly-charged peptides this situation is reversed, and the intramolecular charge “solvation” energy is more negative than the helix formation energy. However, even though the charge “solvation” energy

(53) Wu, J.; Lebrilla, C. B. *J. Am. Chem. Soc.* **1993**, *115*, 3270.

(54) Wu, Z.; Feneslau, C. *J. Am. Soc. Mass Spectrom.* **1992**, *3*, 863. Wu, Z.; Feneslau, C. *Tetrahedron* **1993**, *49*, 9197.

(55) Zhang, K.; Zimmerman, D. M.; Chung-Phillips, A.; Cassady, C. J. *J. Am. Chem. Soc.* **1993**, *115*, 10813.

(51) Mitchell, J. B. O.; Price, S. L. *J. Comp. Chem.* **1990**, *11*, 1217.

(52) The Coulomb energies for a β -sheet were estimated by distributing the charges in their minimum energy configuration around the edges of a rectangle with approximately the dimensions of a β -sheet.

is less negative than the helix formation energy for cytochrome *c*, it is still sufficiently large that charge "solvation" might be expected to play a significant role in defining its structure in the gas phase. Some recent experimental studies support this notion. The free energies for initial hydration of the +5 and +7 charge states of cytochrome *c* have recently been determined from equilibrium constant measurements.⁷ The free energies are much less negative than the free energies for initial hydration of H_3O^+ and GlyH^+ (protonated glycine).^{56,57} If the charge was exposed on the surface of the protein, initial hydration energies comparable to those determined for H_3O^+ and GlyH^+ would be expected. These results indicate that the charge is effectively shielded in at least the +5 and +7 charge states of cytochrome *c*. Thus it appears that intramolecular charge "solvation" must play an important role in defining the structure of these large multiply charged protein ions in the gas phase.

The importance of intramolecular charge "solvation" effects is expected to increase with protein charge. While an α -helix has favorable intramolecular interactions, this geometry cannot provide for effective intramolecular charge "solvation". The geometry that maximizes intramolecular charge "solvation" is a "string of beads", where each bead is a "solvation" shell surrounding a protonated site, and the beads are connected by a short length of unfolded peptide chain. The "string of beads" conformation, however, lacks the additional intramolecular interactions that stabilize an α -helix. Thus the conformations of the higher charge states must result from a compromise between maximizing intramolecular interactions and intramolecular charge "solvation" and minimizing Coulomb repulsion. A string of intramolecular "solvation" shells that also incorporates a substantial number of additional hydrogen bonds and van der Waals contacts is an example of such a conformation. This conformation could also contain helical regions, and another way to think of this geometry is to start with an α -helix and to disrupt it at regular intervals to incorporate intramolecular charge "solvation" shells. Experimentally, we observe that a single unfolded conformation dominates the drift time distributions for all charge states above +9. For the +11 to +13 charge states the cross section of this conformation is close to the one expected for an α -helix (see Figure 7), while for higher charge states it gradually becomes larger. This unfolding is consistent with the gradual unwinding of an α -helix to produce intramo-

lecular charge "solvation" shells and regions of extended peptide string described above. The cross section estimates presented in Figure 7 suggest that even for the highest charge state observed (+20), the cross section of cytochrome *c* is still lower than that expected for a completely extended string, so that a substantial fraction of the residues is still involved in solvating the charge.

Conclusions

Cross sections measured for the low charge states of BPTI are slightly smaller than those estimated for the native solution-phase conformation indicating that the gas-phase protein is slightly more compact than in solution, in agreement with the predictions of molecular dynamics simulations. The cross sections systematically increase with increasing charge, presumably because the protein expands to minimize Coulomb repulsion. The drift time distributions do not change as the injection energy is increased to collisionally heat the protein ions as they enter the drift tube, indicating that BPTI either does not unfold under these conditions or it refolds in less than 100 μs . These results are consistent with the known stability of BPTI where the three-dimensional structure is partially locked into place by three covalent disulfide bridges.

In contrast to BPTI, cytochrome *c* has no disulfide bridges, and so it is relatively free to adopt other conformations in the gas phase. Compact conformations with cross sections close to those estimated for the native structure were only observed for the low charge states. For intermediate charge states conformations as compact as the native form could be generated by electrospraying a neutral solution, but when collisionally heated, these conformations unfold through a series of well-defined intermediates to a more extended conformation. This structural transformation, which is in some respects analogous to acid denaturation in solution, is probably driven by Coulomb repulsion. For the higher charge states only extended conformations are observed. Coulomb repulsion is much more important in the gas phase than in solution, and the changes observed as a function of charge state can be rationalized in terms of the balance between attractive intramolecular interactions and Coulomb repulsion.

Acknowledgment. We gratefully acknowledge the National Science Foundation (Grant No. CHE-9306900) for partial support of this work.

JA9619059

(56) Lau, Y. K.; Ikuta, S.; Kebarle, P. *J. Am. Chem. Soc.* **1982**, *104*, 1462.

(57) Klassen, J. S.; Blades, A. T.; Kebarle, P. *J. Phys. Chem.* **1995**, *99*, 15509.